

Curve modeling in shape spaces

Ian Dryden



Geometry for Anatomy Workshop, BIRS, Banff,
August 29-September 2, 2011

Outline

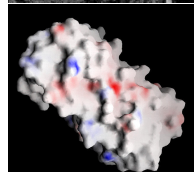
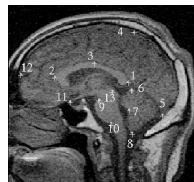
- 1 Introduction
- 2 Shape Curves
- 3 Shape Splines
- 4 Discussion

Outline

- 1 Introduction**
- 2 Shape Curves
- 3 Shape Splines
- 4 Discussion

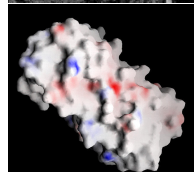
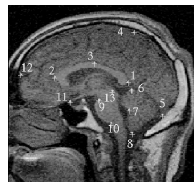
SHAPE

- Geometrical properties that are invariant under certain registration transformations. Some examples...



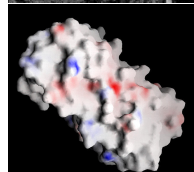
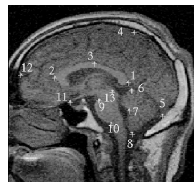
SHAPE

- Geometrical properties that are invariant under certain registration transformations. Some examples...
- Euclidean Shape: point sets which invariant under translation, rotation and scale



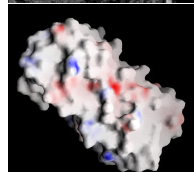
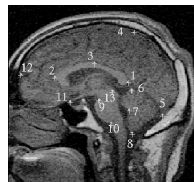
SHAPE

- Geometrical properties that are invariant under certain registration transformations. Some examples...
- Euclidean Shape: point sets which invariant under translation, rotation and scale
- Size-and-shape: point sets which invariant under translation and rotation



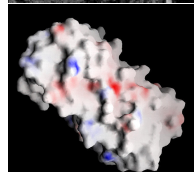
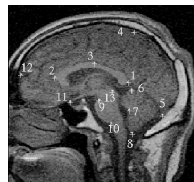
SHAPE

- Geometrical properties that are invariant under certain registration transformations. Some examples...
- Euclidean Shape: point sets which invariant under translation, rotation and scale
- Size-and-shape: point sets which invariant under translation and rotation
- Closed outline shapes: curves which are invariant under diffeomorphic transformations of arc-length.



SHAPE

- Geometrical properties that are invariant under certain registration transformations. Some examples...
- Euclidean Shape: point sets which invariant under translation, rotation and scale
- Size-and-shape: point sets which invariant under translation and rotation
- Closed outline shapes: curves which are invariant under diffeomorphic transformations of arc-length.
- Note: Quotient spaces often appropriate.



Landmark shapes

- EXAMPLE: Object: k points in m dimensions $X \in \mathbb{R}^{km}$
- Transformation group: Translation, rotation and scale.
- Here there are $k = 50$ points in $m = 2$ dimensions.



- Kendall's (1984) shape space: $\Sigma_m^k = \mathcal{S}^{(k-1)m-1} / SO(m)$.
- Quotient space: Pre-shape sphere with rotation removed.

Practicalities: Procrustes matching

We wish to register the man (X_1) on to the fish (X_2), using translation, rotation and scale.

X_1, X_2 are $k \times m$ matrices, which are centered ($\mathbf{1}_k^T X_j = 0$)



X_1



X_2



X_1^P, X_2

Explicit solution: SVD. Procrustes shape distance $d([X_1^P], [X_2])$.

Outline

- 1 Introduction
- 2 Shape Curves**
- 3 Shape Splines
- 4 Discussion

MINIMAL GEODESICS

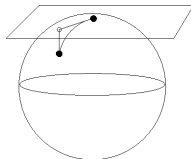
- A PRE-SHAPE has had location and scale removed BUT NOT rotation. It lives on a sphere.

MINIMAL GEODESICS

- A PRE-SHAPE has had location and scale removed BUT NOT rotation. It lives on a sphere.
- Given two pre-shapes μ, z the minimal geodesic between their shapes corresponds to

$$\Gamma(s) = \mu \cos s + z \sin s, \quad 0 \leq s \leq \pi/2$$

where z has been Procrustes rotated to μ .

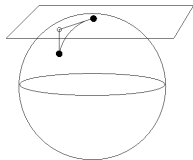


MINIMAL GEODESICS

- A PRE-SHAPE has had location and scale removed BUT NOT rotation. It lives on a sphere.
- Given two pre-shapes μ, z the minimal geodesic between their shapes corresponds to

$$\Gamma(s) = \mu \cos s + z \sin s, \quad 0 \leq s \leq \pi/2$$

where z has been Procrustes rotated to μ .



- Note that this is the horizontal lift of the minimal geodesic in shape space.

EXAMPLE

GEODESIC PATH: Fish \rightarrow Fishman \rightarrow Man



$$\Gamma(s) = \mu \cos s + z \sin s, \quad 0 \leq s \leq \pi/2.$$

EXAMPLE: RAT SKULLS

Bookstein's (1991) rat skull data.

The rats were carefully X-rayed at age N days, where $N \in \{7, 14, 21, 30, 40, 60, 90, 150\}$,

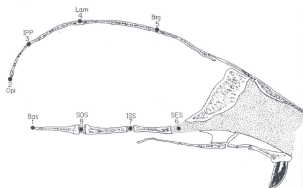
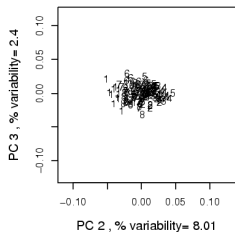
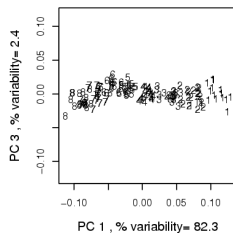
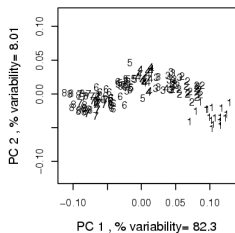


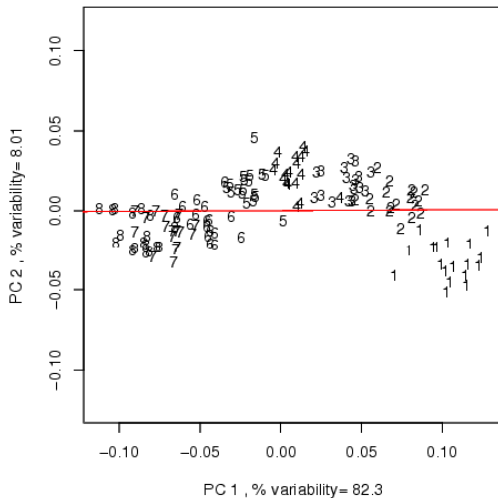
[Image: Bookstein, 1991]

There are $n = 18$ rats with complete sets of $k = 8$ landmarks at each age in $m = 2$ dimensions.

PCA in tangent space



Minimal geodesic



SHAPE CURVE FAMILY

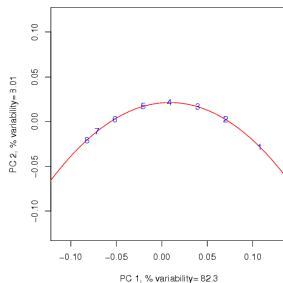
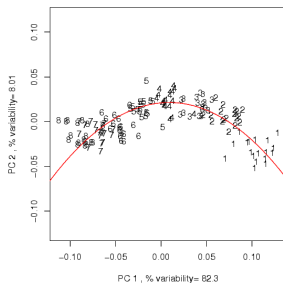
- Joint work with Kim Kenobi and Huiling Le (Nottingham).
- Let us consider an extension by introducing another pre-shape w_2 which is orthogonal to w_1 and μ .
- Also, consider a function $t_1(s)$ which gives the position in the direction w_2 for each s .
- The shape curve lifted to the the pre-shape space is then defined as:

$$\Gamma_{(\mu, w_1, w_2; t_1)}(s) = \cos\{t_1(s)\} \{(\cos s)\mu + (\sin s) w_1\} + \sin\{t_1(s)\} w_2,$$

QUADRATIC SHAPE CURVE

$$t_1(s) = a_0 + a_1 s + a_2 s^2$$

$$\Gamma_{(\mu, w_1, w_2; t_1)}(s) = \cos\{t_1(s)\} \{(\cos s)\mu + (\sin s) w_1\} + \sin\{t_1(s)\} w_2,$$



ESTIMATION

Best fitting curve: Minimise

$$F(\underline{a}) = \sum_{i=1}^g \sum_{j=1}^{n_i} d^2\{[Z_{ij}], \gamma(\hat{s}_i)\}$$

over the parameters \underline{a} , where \hat{s}_i minimises

$$F_{\gamma,i}(s) = \sum_{j=1}^{n_i} d^2\{[Z_{ij}], \gamma(s)\}, \quad i = 1, \dots, g,$$

and $\gamma()$ is the shape corresponding to pre-shape $\Gamma()$, $[Z]$ is the shape of Z , and $d()$ is a shape distance.

PRACTICALITIES

- In practice we often have the shapes of μ , w_1 estimated to be almost identical to the Procrustes mean and the first shape PC.
- The use of the Procrustes mean and shape PCAs gives an excellent approximation in many applications.
- For small s and $t_1(s)$:

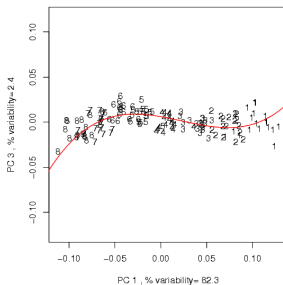
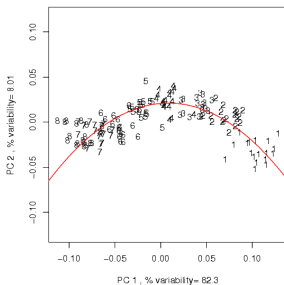
$$\Gamma_{(\mu, w_1, w_2; t_1)}(s) \approx \mu + sw_1 + t_1(s)w_2.$$

QUADRATIC-CUBIC SHAPE CURVE

$$t_1(s) = a_0 + a_1 s + a_2 s^2$$

$$t_2(s) = b_0 + b_1 s + b_2 s^2 + b_3 s^3$$

$$\Gamma_{(\mu, w_1, w_2, w_3; t_1, t_2)}(s) = \cos\{t_2(s)\} \Gamma_{(\mu, w_1, w_2; t_1)}(s) + \sin\{t_2(s)\} w_3,$$



HYPOTHESIS TESTS

In the quadratic-cubic model there are seven free parameters, $\{a_0, a_1, a_2, b_0, b_1, b_2, b_3\}$, which specify the curves. We set up three hypotheses which express the different relationships.

- H_0 : $a_0 = a_1 = \dots = b_3 = 0$ (Geodesic)
- H_1 : At least one of a_0, a_1, a_2 is non-zero and $b_0 = b_1 = b_2 = b_3 = 0$. (Quadratic)
- H_2 : At least one of a_0, a_1, a_2 is non-zero and at least one of b_0, b_1, b_2, b_3 is non-zero. (Quadratic-cubic)

LIKELIHOOD RATIO TEST

- Using a complex Watson model

$$f([z]) \propto \exp(\kappa \cos^2 d([z], [\mu])),$$

gives the log-likelihoods under the three models as

$$l_0 = 4766.26, l_1 = 5040.40, l_2 = 5076.82.$$

Thus $-2(l_0 - l_1) = 548.27$, $-2(l_1 - l_2) = 72.85$.

LIKELIHOOD RATIO TEST

- Using a complex Watson model

$$f([z]) \propto \exp(\kappa \cos^2 d([z], [\mu])),$$

gives the log-likelihoods under the three models as

$$l_0 = 4766.26, l_1 = 5040.40, l_2 = 5076.82.$$

Thus $-2(l_0 - l_1) = 548.27$, $-2(l_1 - l_2) = 72.85$.

- Comparing these statistics with a χ_3^2 and a χ_4^2 distribution respectively shows that each reduction in the sum of squares is highly significant.

LIKELIHOOD RATIO TEST

- Using a complex Watson model

$$f([z]) \propto \exp(\kappa \cos^2 d([z], [\mu])),$$

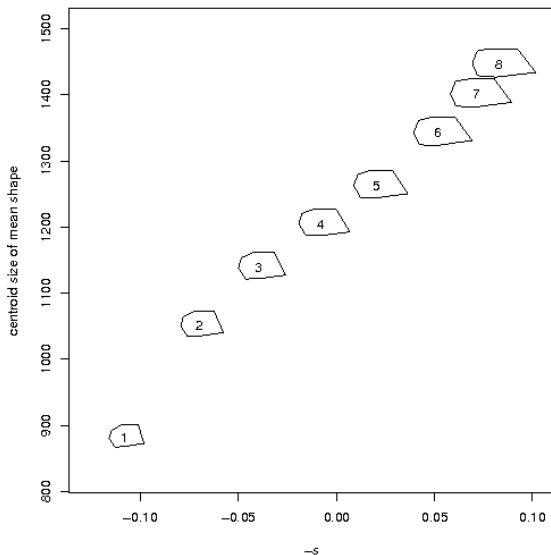
gives the log-likelihoods under the three models as

$$l_0 = 4766.26, l_1 = 5040.40, l_2 = 5076.82.$$

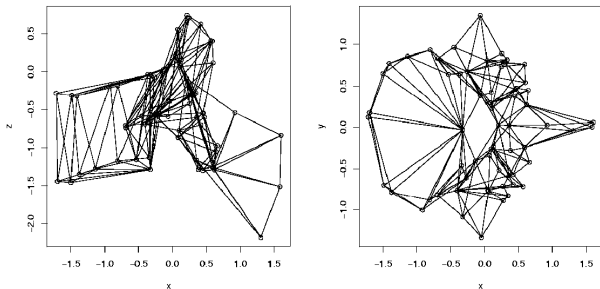
Thus $-2(l_0 - l_1) = 548.27$, $-2(l_1 - l_2) = 72.85$.

- Comparing these statistics with a χ_3^2 and a χ_4^2 distribution respectively shows that each reduction in the sum of squares is highly significant.
- There is strong evidence against the geodesic and quadratic models in favour of the quadratic-cubic model.

GROWTH ALONG THE QUADRATIC-CUBIC CURVE



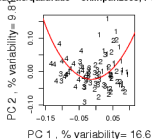
ANOTHER EXAMPLE: HOMINIDS



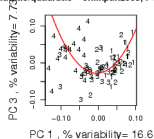
Lumbar vertebra 1-4. Chimpanzee, Gorilla, Human.
 $k = 62$ landmarks in $m = 3$ dimensions, $n = 22$ per group.
Data from Paul O'Higgins.

VERTEBRA

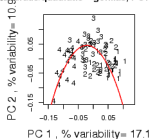
Quadratic - quadratic - chimpanzees, PC1 vs PC2



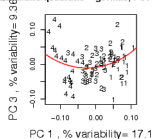
Quadratic - quadratic - chimpanzees, PC1 vs PC3



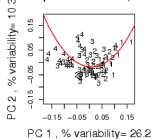
Quadratic - quadratic - gorillas, PC1 vs PC2



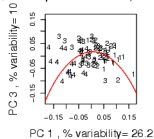
Quadratic - quadratic - gorillas, PC1 vs PC3



Quadratic - quadratic - humans, PC1 vs PC2



Quadratic - quadratic - humans, PC1 vs PC3



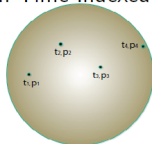
Outline

- 1 Introduction
- 2 Shape Curves
- 3 Shape Splines**
- 4 Discussion

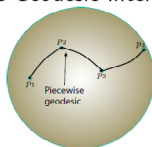
SAMSI AOOD program, North Carolina

- Joint work with Jingyong Su, Anuj Srivastava and Eric Klassen (Florida State) and Hailing Le (Nottingham).
- Consider points p_i on manifold M at times t_i , $i = 1, \dots, n$.

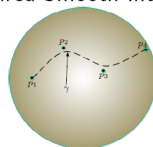
Given Time-Indexed Data



Piecewise-Geodesic Interpolation



Desired Smooth Interpolation



Motivating example

Sequence of outlines of a dancer: 100 points located on outline in 2D.

- Translation, rotation and scale invariance.
- Manifold is Kendall's shape space (complex projective space).

Motivating example

Sequence of outlines of a dancer: 100 points located on outline in 2D.

- Translation, rotation and scale invariance.
- Manifold is Kendall's shape space (complex projective space).
- Either: interpolate between data points (here shapes in 2D)



Motivating example

Sequence of outlines of a dancer: 100 points located on outline in 2D.

- Translation, rotation and scale invariance.
- Manifold is Kendall's shape space (complex projective space).
- Either: interpolate between data points (here shapes in 2D)



- Or: smooth a noisy sequence of shapes

Roughness penalty approach

- Find an optimal path $\hat{\gamma}$ by minimizing

$$\frac{\lambda_1}{2} \sum_{i=1}^n d(\gamma(t_i), p_i)^2 + \frac{\lambda_2}{2} \mathcal{R}(\gamma).$$

- Example roughness penalty: $\mathcal{R}(\gamma) = \int_0^1 \left\langle \frac{D^2\gamma}{dt^2}, \frac{D^2\gamma}{dt^2} \right\rangle dt$.
Objective function: Data term and Smoothing term.

$$S = \lambda_1 E_d + \lambda_2 E_s.$$

- Using the Palais metric an explicit expression for the gradient is obtained, leading to a practical fitting algorithm.
- Can use cross-validation to choose λ_2/λ_1 .

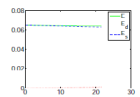
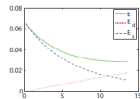
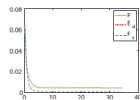
Video dancer



Real sequence

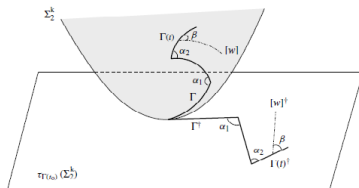


Initial path

 $\lambda_1 = 0.1, \lambda_2 = 1$  $\lambda_1 = 1, \lambda_2 = 1$  $\lambda_1 = 100, \lambda_2 = 1$ 

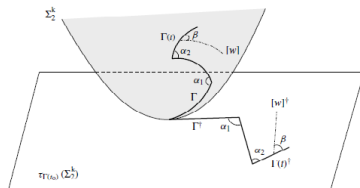
OTHER APPROACHES

- Unrolling and unwrapping splines: Kume et al. (2007)



OTHER APPROACHES

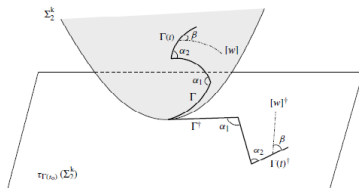
- Unrolling and unwrapping splines: Kume et al. (2007)



- Geodesic curves: Le and Kume (2000). Principal geodesics: Huckemann et al (2010), Fletcher et al. (2004)

OTHER APPROACHES

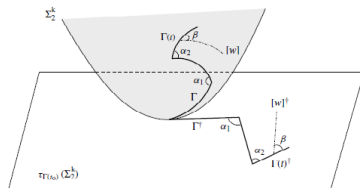
- Unrolling and unwrapping splines: Kume et al. (2007)



- Geodesic curves: Le and Kume (2000). Principal geodesics: Huckemann et al (2010), Fletcher et al. (2004)
- Tangent space functional curves: Kent et al. (2001)

OTHER APPROACHES

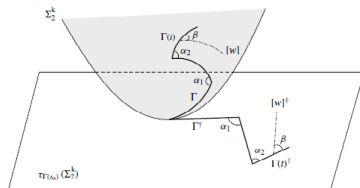
- Unrolling and unwrapping splines: Kume et al. (2007)



- Geodesic curves: Le and Kume (2000). Principal geodesics: Huckemann et al (2010), Fletcher et al. (2004)
- Tangent space functional curves: Kent et al. (2001)
- Principal nested spheres: Jung et al (2011)

OTHER APPROACHES

- Unrolling and unwrapping splines: Kume et al. (2007)



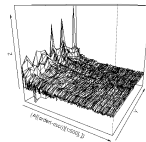
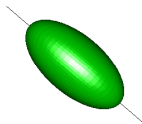
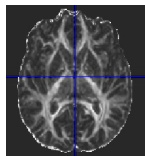
- Geodesic curves: Le and Kume (2000). Principal geodesics: Huckemann et al (2010), Fletcher et al. (2004)
- Tangent space functional curves: Kent et al. (2001)
- Principal nested spheres: Jung et al (2011)
- Local Polynomial Regression: Yuan et al (2011)

Outline

- 1 Introduction
- 2 Shape Curves
- 3 Shape Splines
- 4 Discussion**

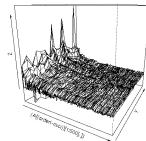
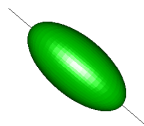
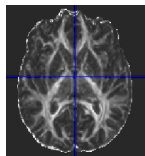
Discussion

- Many other types of non-Euclidean data, high-dimensional, requiring new statistical methodology.



Discussion

- Many other types of non-Euclidean data, high-dimensional, requiring new statistical methodology.



- Statistics/biology/computer science/mathematics/other bridges

Further information

- Kenobi, K., Dryden, I.L. and Le, H. (2010). Shape curves and geodesic modelling *Biometrika*. **97** (3): 567-584.
- J. Su, I. L. Dryden, E. Klassen, H. Le and A. Srivastava (2011). Fitting Smoothing Splines to Time-Indexed, Noisy Points on Nonlinear Manifolds. *Submitted to Journal of Image and Vision Computing*

Further information

- Kenobi, K., Dryden, I.L. and Le, H. (2010). Shape curves and geodesic modelling *Biometrika*. **97** (3): 567-584.
- J. Su, I. L. Dryden, E. Klassen, H. Le and A. Srivastava (2011). Fitting Smoothing Splines to Time-Indexed, Noisy Points on Nonlinear Manifolds. *Submitted to Journal of Image and Vision Computing*
- Support: EPSRC, Leverhulme Trust, SAMSI



Thank you!

Palais Metric

- Samir et al. (2011) used the Palais metric for computing the gradient of the objective function S .
- Let γ be a twice differentiable path in manifold M and let v, w be two smooth vector fields along γ , i.e. $v(t), w(t) \in T_{\gamma(t)}(M)$ for $t \in [0, 1]$. Then, the second-order Palais (1963) metric is:

$$\langle v(0), w(0) \rangle_{\gamma(0)} + \left\langle \frac{Dv}{dt}(0), \frac{Dw}{dt}(0) \right\rangle_{\gamma(0)} + \int_0^1 \left\langle \frac{D^2v}{dt^2}, \frac{D^2w}{dt^2} \right\rangle_{\gamma(t)}$$

- The explicit form of the gradient is useful for in a practical algorithm for fitting the spline.